The Vasoproliferative Phase in the Oxygen-Induced Rat Model of Retinopathy of Prematurity Exhibits Concomitant Increased Expression of VEGF164 and Phosphorylation of eNOS at Serine1179.

Jorge L Jacot[1,2*], Robin C Looft-Wilson[3], Nazita Yousefieh[4], Frank A Lattanzio[5], Alireza Hosseini[5]

[1]Department of Pathology and Anatomy, Eastern Virginia Medical School, USA
[2]Angioceutics International LLC, USA
[3]Department of Kinesiology and Health Sciences, College of William and Mary, USA
[4]Jones Institute for Reproductive Medicine, Department of Obstetrics and Gynaecology, USA
[5]Department of Physiological Sciences, T.R. Lee Center for Ocular Pharmacology, Eastern Virginia Medical School, USA

Abstract

Purpose: The nitric oxide pathway requires phosphorylation of eNOS to liberate NO. We correlated mRNA/protein levels of VEGF164, and phosphorylated Serine1179 of eNOS during ROP vasoproliferation. Methods: Animals were exposed to oxygen (50/10% every 24-hours) for 14 post-natal (PN) days. Pups were continuously exposed to 20.9% ambient oxygen from PN15 and enucleated on PN days 15, 18, and 20. ADPase stained retinas were analyzed for degree of avascularity/total retina area. Western-blotting quantified the phosphorylation of eNOS at Ser^{1179}, the ratio of total eNOS to ERK2. Immunoreactivity of VEGF and of eNOS serine1177 determined tissue protein expression. Results: Percent retinal avascularity was reduced ($p<0.05$) from 39.69% to 28.79%, to 18.53%, for PN days 15, 18, and 20, respectively, with elevations of VEGF mRNA, and eNOS. Phosphorylation of eNOS at Ser1179 was greater at PN20 than PN15 and control. Immunoreactivity of VEGF and eNOS increased. Conclusion: Findings provide insight into mechanisms involving specific interrelationships between VEGF and phosphorylated eNOS in the vasoproliferation of ROP.

Keywords: Retinopathy of prematurity, ROP, Nitric oxide, NO, Vascular endothelial growth factor, VEGF.

Accepted on January 30, 2017

Introduction

The molecular mechanisms governing angiogenic remodelling of the retina in retinopathy of prematurity (ROP) are multi-faceted, complex and have not yet been fully elucidated. The use of animal models for mechanistic studies of ROP has demonstrated several obligatory signaling molecules and transduction pathways in the etiology of the disease. However, despite these revelations, the elements within the highly orchestrated angiogenic signaling of the distinct phases of ROP remains enigmatic and the successful clinical management of the disease continues to be difficult.

In the realm of clinical practice, ROP is an iatrogenic disease. The intervention treatment for pulmonary insufficiency of pre-term neonates is to place them on high oxygen therapy. Regrettably, this establishes a milieu of retinal hypoxia when the neonate is weaned from the high oxygen. The retinal hypoxia is mediated as a consequence of arrest in retinal vascular development in response to high oxygen tension at the level of the retina. In humans (and in the OIR rat model) this sequela renders the mid- and peripheral retina avascular. Consequently, when the neonate is placed in ambient oxygen the ensuing retinal hypoxia up-regulates HIF1-alpha which is an upstream mediator for the up-regulation of VEGF expression. This increased VEGF expression contributes to angioproliferation (the vasoproliferative hypoxic phase of ROP).

Downregulation of vascular endothelial growth factor (VEGF) has been implicated in the arrest or obliteration of blood vessels during hyperoxia [1]. In the setting of hypoxia, upregulation of VEGF has been demonstrated to play a central role in the retinal vasoproliferative response. The transcriptional activation and magnitude of the hypoxia-induced upregulation of VEGF by the hypoxia inducible factor-1 alpha (HIF-1α) has been well documented in cultured hypoxic cells [2]. Other molecules have been shown to modulate the angiogenic response by interacting with VEGF upstream or downstream and thereby influencing the extent of arrest or vasoproliferation.

The free radical nitric oxide (NO) has been reported to exhibit either direct antagonistic effects or direct facilitation on the angiogenic process. Furthermore, NO also interacts with VEGF to regulate the potent angiogenic response mediated by VEGF as well as promote permeability of microvessels [3]. Crucial to the understanding of the characteristic vascular remodelling of ROP vasculopathy is the complex interplay between VEGF and NO signaling. For instance, the induction of *VEGF* gene expression can be regulated by NO-mediated activation of HIF1-α and VEGF acting as an eNOS agonist can promote vascular remodelling and angiogenesis [4]. However, because the reported effects of NO on angiogenesis are discordant, investigators lack unanimity on the extent that NO contributes to the vasculopathy of ROP. The lack of conclusive pre-clinical data on the pathogenic contribution of NO to ROP vasculopathy

inhibits a decision regarding the application of NO modulators for the clinical management of ROP.

Overexpression of eNOS has been reported to promote angiogenesis, as well as vascular closure. The eNOS overexpressing transgenic mouse model of oxygen-induced retinopathy (OIR) [5] can, in the absence of VEGF signaling, promote pathologic angiogenesis and facilitate angioproliferative drive. However, during hyperoxia eNOS can produce superoxide anion (O_2^-) and peroxynitrite ($ONOO^-$) in response to a hyperoxia-mediated deficiency in tetrahydrobiopterin (BH4) and these radical metabolites then promote apoptosis-mediated vessel closure as reported by Edgar et al. Reported discrepancies on contributions by NO to the vascular manifestations of ROP stem from variations in the type of NO inhibitor used, the tissue concentration of NO, the isoform source of the NO production, the existence of genetic polymorphisms, the oxygen concentration, the stage of the disease, and the selection of the altered NOS isoform in a transgenic animal model [5].

VEGF-mediated angiogenesis requires the formation of NO from activated eNOS via distinct pathways. The eNOS-VEGF pathway provides cell survival, proliferation, and differentiation signals of endothelial progenitor cells. Signaling via this pathway requires the phosphorylation of Akt from PI3K and the subsequent phosphorylation of eNOS by Akt to liberate NO and may involve silent information regulator 1 (SIRT1) [6]. Upon VEGF signaling in HUVEC cells, activation of eNOS is regulated by transient phosphorylation at Serine1177 (pSer1179-eNOS is the rat homolog of human Serine1177) mediated via VEGF-induced Akt protein kinase activation [7]. Reciprocally, eNOS can be inhibited by dephosphorylation at Serine1177 via VEGF-mediated activation of PKC which preferentially phosphorylates Threonine497.

NO appears to play a role in the severity, and perhaps etiology, of human ROP. Subretinal fluid from stage 5 ROP patients exhibits the ability to induce NO production from pro-inflammatory M1-type macrophages grown *in vitro*, induces endothelial cord formation and has a composition of elevated VEGF-A and other cytokines which is both pro-angiogenic and pro-inflammatory [8]. Insights gained from experimental inquiries into the involvement of NO in established and relevant animal models of ROP could open up opportunities for rational development of future therapeutic molecular targets for disease management.

The current study temporally correlates the endogenous mRNA and protein levels of VEGF164 and bioactive phosphorylated Serine1179 eNOS in the vasoproliferative phase of the rat model of oxygen-induced retinopathy (OIR). Our results suggest that a pro-angiogenic milieu is established in the presence of both elevated VEGF, as well as bioactive eNOS levels. Elevated bioactive eNOS was obtained during the vasoproliferative phase in the OIR rat model.

These findings provide insight into possible operant mechanisms in the vasoproliferation of ROP and may therefore be useful for development of future therapeutic modalities aimed at the management of pre-term neonates in the intensive care unit at risk for the development of ROP.

Research Design and Methods

Animal studies

We used an established rat model of ROP; a historical perspective of this animal model has been given by [9]. Timed-pregnant Sprague-Dawley rats carrying pups of approximately 15 days gestation were obtained from the vendor (Charles River, Laboratories, Raleigh, North Carolina). Upon delivery to our institution, the pregnant dams were allowed to acclimate without manipulations while housed in standard shoebox cages with *ad libidum* water and food until they gave birth. Litters from different mothers were co-mingled in the oxygen chamber to have available a genetically heterogeneous cohorts of 16 pups fed by a single dam. This ratio of dam to nursing pup provides the appropriate stress level and exhibits a delay in weight gain compared to littermate naïve pups housed with surrogate dams in ambient oxygen which serve as controls. Within several hours following birth, the mother and offspring pups were placed in the oxygen chamber. The environment within the oxygen chamber was adjusted to 50% oxygen for the first 24 hours post-natal. After 24 hours, the oxygen concentration was rapidly reduced to 10%, where it remained for the subsequent 24 hours. The oxygen levels cycled between 50% and 10% fraction of inspired O_2 concentration (FiO_2), every 24 hours for the first 14 days post-natal. This particular pattern of oxygen fluctuation was derived by Penn et al to emulate, in the rat model, the systemic arterial blood gas concentrations typical of a pre-term neonate in the ICU [10]. Surrogate lactating mothers were introduced and alternated in the chamber with the pup litter during the 14 day period as needed to assure that stress levels of the mothers did not adversely affect their ability to lactate and to adequately nourish the pups.

On post-natal day 15, rats were removed from the chamber and exposed to ambient oxygen (20.9%) for completion of vascular development. During ambient normoxia exposure, the retina is rendered "*hypoxic*", presumably linked to the extent of retinal avascularity established during the oscillating oxygen phase. Rat pups were euthanized and bilaterally enucleated on days 15, 18, and 20 post-natal (n=15 to 16/time point). The use and handling of the animals in this study conformed to the NIH Guide for the Care and Use of Laboratory Animals (No. 85-23), Institute of Laboratory Animal Resources, Commission on Life Sciences, National Research Council (Washington, D.C.). The association for research in vision and ophthalmology (ARVO) statement for the use of animals in ophthalmic and vision research. All animal experiments adhered to protocols approved by the institutional animal care and use committee (IACUC) of Eastern Virginia Medical School, Norfolk, Virginia.

Morphometric measurements of the retinal vascular network

The extent of retinopathy progression can be slightly asymmetrical, but involvement is comprehensively bilateral in this animal model. Therefore, a single retina from each rat underwent morphometric analysis to assess microangiopathic changes and the contralateral retina was used for a series of molecular analysis as described elsewhere in this paper. For morphometric analysis, an eye from each rat was fixed in 10% paraformaldehyde for 30 minutes before the eye was dissected.

The retina was then isolated and processed for a retinal whole-mount preparation. The isolated retina was transferred to fresh 10% paraformaldehyde for an overnight fix. The retinal vessels were histochemically stained using a nonspecific adenosine diphosphatase (ADPase) enzyme technique described by [11,12]. This ADPase staining will identify segments of viable microvessels that exhibit phosphatase activity.

Digital images of flat-mounted whole-mounts of ADPase stained retinal vasculatures from each rat were analyzed at 15, 18, and 20 days post-natal time points. Images were captured using an Olympus CKX41 inverted microscope with a 1.25x objective coupled to a digital camera (Olympus DP-71). Using a PhotoShop Image Analysis System and a Wacom Digitizer Tablet, the total retinal area, the area of vascularity and the area of avascularity were manually delineated from the flat-mounted images of each dissected retina. The calibrated pixel dimension obtained in PhotoShop was converted to mm^2 area of the retina and expressed as percent of avascular or vascular area from the total retina area. All measurements where conducted under double-masked conditions to minimize any potential bias. Although the actual tracing was made by a single investigator to optimize consistency, the accuracy of the tracings was confirmed by an additional masked investigator. No discrepancies as to the accuracy of the tracings were observed between investigators which would have required a retracing of the sample in question.

Method for quantitative evaluation of growth factor

The contralateral retina from each neonate pup was assigned to be evaluated for VEGF and eNOS mRNA levels at each of the three designated time points. The dissected retinas were placed in 10 µl of RNAlater® (ThermoFisher Scientific) and were frozen on dry ice. Real time reverse transcriptase polymerase chain reaction (real time rtPCR) technique was used to determine the retinal VEGF and eNOS mRNA levels. VEGF primers were designed based on Gen Bank accession number (M32167) with the following sequence (Forward 5'-ACC AGC GCA GCT ATT GCC GT; Reverse 5'-CAC CGC CTT GGC TTG TCA CA). The eNOS primers were (Forward 5'-CTT CCG AAG CTT CTG GCA ACA GCC ACA ATT) and (Reverse 5-GGA CTC AGA TCT AAG GCG GTT GTT CAC TTC). (Real-time PCR primer and probes Database, ID:3944). Beta Actin was used as a housekeeping gene (Qiagen, Frederick, MD, USA. Catalog#: PPRO6570C). The RNA was extracted in Trizol (Life technologies, Grand Island, NY) and purified using RNeasy kit (Qiagen, Valencia, CA). The validity of this primer sequence has been documented in another study [13].

Method of Western blot analysis for phosphorylation of eNOS

Dissected retinas were fresh frozen immediately on dry ice for Western-blotting to quantify the relative phosphorylation of eNOS at Ser1179 (pS1179eNOS), the ratio of total eNOS to a reference gene (ERK2). Tissues were homogenized in 200 µl lysis buffer with phosphatase inhibitors (50 mM Tris-HCl, 100 mM NaF, 15 mM Na4P2O7, 1 mM Na3VO4, 1% Triton X-100, and 1:200 protease inhibitor cocktail solution (#P2714, Sigma, St. Louis, MO); pH=7.6), incubated for 1 hr at 4°C, and centrifuged (14,000 rpm, 10 min) to remove insoluble material. Proteins were separated by 10% SDS-PAGE (4% stacking gel) using 45 µg or 50 µg of protein for a given membrane (with exceptions for two samples in which only 20 µl and 11 µl could be loaded). Two samples from each group were loaded onto each gel (Total of 4 gels; 7-8 samples each group; two samples were duplicates from the same animal, one in the control group and one in the Oxygen P15 group, so these were each averaged and treated as one sample in the graph).

Proteins were transferred to a nitrocellulose membrane using electro-blotting (45 min). Membranes were cut into 3 sections, with a cut just below the 75 KDa marker and just above the 50 KDa marker. The top portion (highest molecular weights) was labelled first for pS1179eNOS (mouse monoclonal antibody, 1:1000, #612393; BD Biosciences, San Jose, CA), followed by HRP-conjugated secondary antibody (anti-mouse IgG, 1:5000, #NA931, GE Healthcare, Piscataway, NJ) and the 140kDa band was visualized with enhanced chemiluminescence (Pierce Biotechnology, Rockford, IL) captured on film. The membrane was then stripped for 15-20 minutes (Restore Western Blot Stripping Buffer, Thermo Scientific, Waltham, MA), and re-probed with eNOS (mouse monoclonal antibody, 1:1000, #610297; BD Biosciences), using the same procedure as with the phosphorylated forms. We have previously shown that this stripping protocol results in negligible residual labelling of the phosphorylated form, even with long film exposure times [14].

The bottom portion of the membrane was labelled for ERK2 (rabbit polyclonal antibody, 1:1000, #sc-154; Santa Cruz Biotechnology, Inc., Dallas, TX) using a near-infrared-conjugated secondary antibody [goat anti-rabbit IRDye® 680RD, #926-68171, 1:20,000; LiCor Biotechnology, Lincoln, NE) and a LiCor Odyssey Sa infrared imaging system to visualize the 42KDa band. ERK2 (also called MAPK1) has been reported to be a reliable reference gene for rat retinas during development from days E18-P45 [15].

Immunohistochemistry

The dissected globe was placed in 10% buffered paraformaldehyde (1:5 tissue to volume ratio) and were processed for paraffin embedding and cut to yield 5 micron thickness sections (Sakura VIP Processor, AO 812 microtome). Multiple retinal sections from the para-sagittal plane of the globe were used for evaluating the immunohistochemical results. Tissue sections were placed on silanized slides, allowed to air dry and subsequently placed in a 60°C drying oven overnight. Deparaffinized slides were exposed to 3% hydrogen peroxide followed by antigen unmasking with citrate buffer (10 mM citric acid, 0.05% Tween 20, pH 6) in a pre-heated steamer (95°C to 100°C) for 30 minutes. Slides were cooled for 25 minutes prior to staining. Between each procedural step, tissue slides were immersed in two consecutive 5 minute duration rinses of either phosphate buffered saline or distilled water, depending on the particular step. Tissue sections were blocked with 2.5% normal horse serum (Vector Laboratories, Burlingame, CA) for 40 minutes to minimize non-specific antibody binding. Sections were incubated overnight at 4°C with primary antibodies at a 1:50 dilution for VEGF (NB100-698, Novus Biologicals, Littleton, CO). This VEGF antibody is a rabbit polyclonal with cross-reactivity to the splice variants of rat VEGF. The eNOS is a rabbit polyclonal antibody corresponding to a sequence near the C-terminus of endothelial NOS (ADI-905-386, Enzo Life

Sciences, Farmingdale, NY) which cross-reacts with rat and was used at a 1:70 dilution. The antibody to the phosphorylated eNOS is a rabbit polyclonal IgG that is purified using an epitope-specific synthetic phosphopeptide corresponding to phosphorylation site of human serine1177 (ab75-639, Abcam, Cambridge, MA) which cross-reacts with rat and was used at a 1:50 dilution. Negative controls comprised the omission of primary antibodies. Double-stain preparations for eNOS and phosphorylated eNOS immunoreactivity were performed for each slide. The ImmPRESS™ micropolymer reporter enzyme staining system (Vector Laboratories) conjugated to an affinity purified and cross-adsorbed secondary rabbit antibody was used to optimize sensitivity and reduce background. Tissues were incubated in the ImmPRESS™ solution for 40 minutes. The ImmPRESS™ detection kit with the addition of different chromogens was used for visualization. Diaminobenzidene (DAB) chromogen produces a dark brown reaction product and was used to visualize eNOS retinal immunoreactivity. The ImmPRESS™ horseradish peroxidase (HRP) polymer yields a blue reaction product and was used to visualize retinal immunoreactivity of VEGF and phosphorylated eNOS. Slides were subsequently cover slipped using crystal mounting medium (Crystal Mount™, Sigma, Saint Louis, Missouri).

Data Analysis

The mean and standard deviation were determined for all the end points. Statistical analysis with an alpha of $p<0.05$ was considered significant. For western blotting, pS1179eNOS and eNOS, protein bands were quantified by scanning the film and determining the density of each band using Image J software (NIH). Single bands were detected on the membranes at the appropriate size of 140 KDa for both pS1179eNOS and eNOS. pS1179eNOS protein was normalized to total eNOS protein and this ratio was normalized to the control values in each blot to determine the relative change in eNOS phosphorylation with each different treatment, and to allow combining of different blots. It would have been ideal to use a single control sample as a reference on each blot, but the very limited amount of protein in each retina sample made this infeasible. The ERK2 protein bands were evaluated using the quantification tool within the LiCor Odyssey imaging system software package. ERK2 bands appeared at the expected 42 KDa size. Statistics were performed using Prism software (GraphPad Software, Inc., San Diego, CA). Treatments were compared by one-way ANOVA (Bonferroni *post-hoc* analysis).

Results

Flat-mounted whole-mounts of ADPase stained OIR rat retinas showed extensive vascular changes compared to age-matched naïve rat pups, which were exposed only to ambient oxygen. The rats raised in oscillating oxygen concentrations from 10% to 50% of inspired oxygen (FiO_2) every 24 hours for the first 14 days postnatal exhibited a peripheral retina devoid of blood vessels. The peripheral region of avascularity is similar to that observed in human ROP, with the exception that perhaps in the rat vasoproliferative *arrest* (or "vasoattenuation") rather than "vaso-obliteration" appears to be the mechanism by which avascularity in the peripheral retina develops (John Penn personal communications). Computer-assisted morphometric evaluations of the retinal vasculature calculated an average area (n=10) of peripheral avascularity relative to total retinal area of 39.69% ± 11.16% (SD) on post-natal day 15, at the time that the rats had been exposed to ambient oxygen for 24 hours. On post-natal day 18, when rats had been exposed to ambient oxygen for 96 hours, the region of avascularity (n=11) was 28.79% ± 14.75% (SD), a statistically significant difference ($p<0.05$) from post-natal day 15. On post-natal day 20 after 144 hours of ambient oxygen exposure, the region of avascularity (n=11) was 18.53% ± 9.47% (SD), a statistically significant reduction from both post-natal days 15 and 18. Therefore, during the ambient oxygen phase (days 18th to day 20th post-natal) the angioproliferative response and vasculopathy was observed to be at maximum. Numerous vascular tufts, as well as areas of haemorrhages in the region where the peripheral vascular front interfaced with the region of avascularity, were observed. Increased venous vessel tortuosity and dilated capillary meshwork were a characteristic finding in the retinas exposed to oscillating oxygen. The hyaloid vessels were prominent and present in both the oxygen treated and naïve experimental groups. The naïve rat pups exposed only to ambient oxygen throughout the experimental paradigm exhibited a normal and fully vascularized retina at all examined time points (Figure 1).

Change in retinal avascularity in oxygen induced rat model of retinopathy of prematurity at ambient air

Data obtained from real time RT PCR using homogenates of isolated retinas demonstrates a progressively elevated expression of VEGF mRNA and eNOS at post-natal days 15, 18, and 20 over naïve controls (Figures 2 and 3). The progressive rise in mRNA VEGF levels were 1 to 3 fold over normalized control

Figure 1. *Representative vascular appearance of ADPase stained retinal wholemounts in naïve control and at post-natal day 15 (B), post-natal day 18 (C), and post-natal day 20 (D) of oxygen treated rats after transfer to ambient oxygen on post-natal day 14. Note the holangiotic appearance of the naïve rat retina (A) exhibiting a normal appearance of the arterioles, venules, capillary bed, and remnant of the hyaloid vessels emanating at the optic nerve head. The oxygen treated rats (B, C, D), exhibited varying extent of peripheral retinal avascularity with formation of vascular tufts, regions of punctate haemorrhages, vessel tortuosity, and dilated vascular meshworks.*

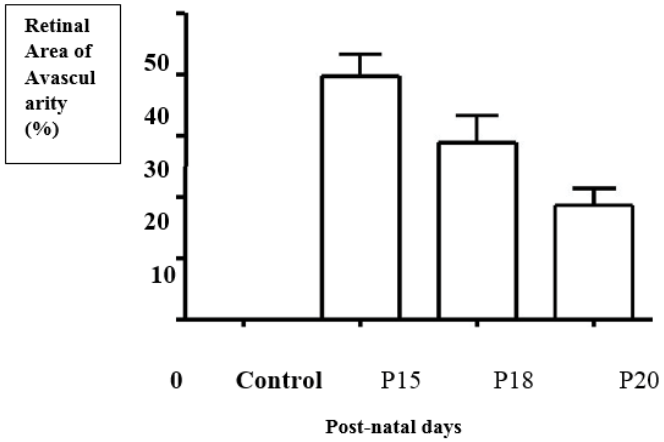

Figure 2. *Calculated average area of peripheral avascularity relative to total retinal area during ambient oxygen phase (days 15, 18, 20 post-natal) in rats (n=10 to 11) exposed to oxygen oscillation for 14 days and in age-matched naïve sibling rat pups exposed only to ambient oxygen. The percent avascularity was significantly reduced ($p<0.05$) from 39.69% ± 11.16 (SD), to 28.79% ± 14.75 (SD), and to 18.53% ± 9.47 (SD), for post-natal days 15, 18, and 20, respectively. The results demonstrate a significant and progressive retinal vasoproliferation (the reciprocal of the area of avascularity) that occurs during the hypoxia-mediated transition to ambient oxygen (20.9%) exposure.*

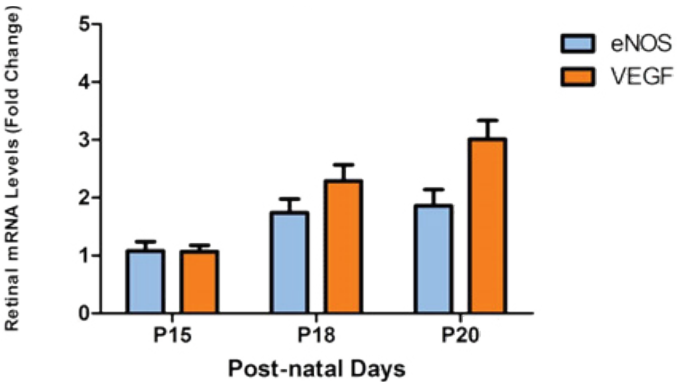

Figure 3. *Retinal mRNA levels of VEGF and eNOS in rat model of retinopathy of prematurity measured by real time RT PCR, normalized to controls.*

levels at the various time points. The rise in eNOS mRNA is of the same magnitude as the rise in VEGF mRNA at post-natal day 15 (1x fold over normalized control) and exhibits a continued increased in levels at day 18 which appears to plateau by day 20. The elevated mRNA expression of both VEGF and eNOS is consistent with a pro-angiogenic milieu coincident with the peak period of vasoproliferation.

Immunohistochemical data support the RT PCR mRNA data with increased immunoreactivity of VEGF and eNOS protein expression localized to various layers of the retina (Figure 4). The VEGF and eNOS mRNA levels are reflective of the bioavailable protein levels of VEGF and eNOS in the retina. The temporal characterization of the expression levels of VEGF and eNOS mRNA, as well as of VEGF and eNOS protein immunoreactivity, correlates with the progression of the ROP vasculopathy that was quantified in computerized analysis of retinal vascular whole-mounts.

Phosphorylation of eNOS at Ser1179 was significantly greater at P20 than P15 and control. However, total eNOS was not different at any time-point, when normalized to the reference gene ERK2. This indicates that although eNOS immunoreactivity in the vasculature of the ganglion cell layer increased with oxygen treatment, total retinal eNOS expression did not.

Discussion

Based on the work of others, we surmise the following operant mechanism(s) to be associated with the vasoproliferative phase of ROP in the rat model of OIR. As a consequence of the avascularity of the peripheral retina established during the exposure to oscillatory oxygen levels, the physiological conditions are set to render the peripheral retina hypoxic (due to high retinal metabolic demands) once the rat is placed in ambient oxygen (20.9% oxygen). A principal effect of this hypoxic stimulus is the reduction of proteosomal degradation of HIF-1 α, thereby increasing its stability and availability for a biological effect on downstream effectors such as VEGF-A [16]. Studies in the OIR mouse model have shown that upon transferring pups from hyperoxia to ambient room air, HIF-1 α and HIF-2 α protein levels are acutely and significantly upregulated within two hours and remain elevated for at least 24 hours for HIF-1 α and for 5 days for HIF-2 α [17]. However, prior work investigating the relationship between the extent of avascularity and the subsequent neovascular response failed to establish a straightforward relationship. Rats maintained at a constant hyperoxic exposure produced extensive avascularity but produced the least neovascular response after four days in room air. Therefore, it was concluded that "avascularity may not be the single overriding stimulus for neovascularization in oxygen induced retinopathy" [18]. This statement is consistent with a complex etiology of the angioproliferative drive, rather than a simple upregulation of VEGF expression driven by HIF-alpha upregulation subsequent to a hypoxia stimulus stemming from avascularity.

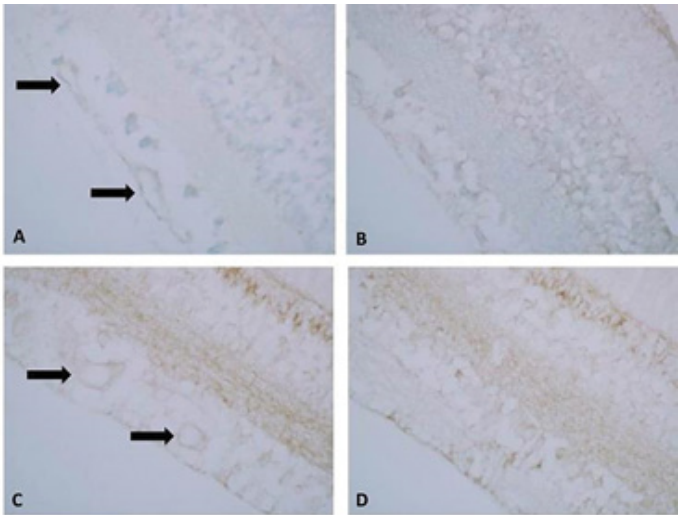

Figure 4. *Immunoreactivity of VEGF and eNOS on retinal cross-sections. Increased immunoreactivity (A) for VEGF is visualized in an oxygen treated rat with Horseradish Peroxidase (HRP) polymer (blue reaction product) over corresponding naïve control (B). Increases of VEGF protein expression are found in the cross-sectioned vessels of the ganglion and nerve fiber layer (black arrows). Visualization of eNOS immunoreactivity with diaminobenzidene (DAB) chromogen (brown reaction product) in oxygen treated rats (C) relative to corresponding naïve control (D). The eNOS immunoreactivity between oxygen treated rats and naïve controls revealed a slight increase in eNOS immunoreactivity with oxygen treatment (C) predominantly in the vasculature of the ganglion cell layer (black arrows).*

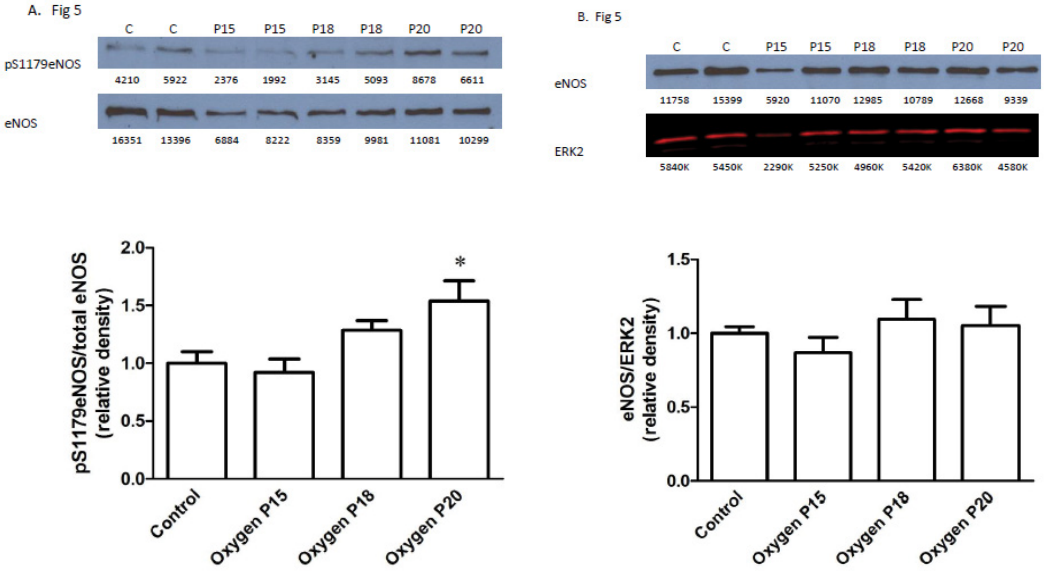

Figure 5. *Phosphorylation of eNOS at Ser 1179 (pS1179eNOS) was greater at 6 days after termination of oxygen treatment (P20), but total eNOS was not different. (A) The relative ratio of pS1179eNOS to total eNOS protein (n=7-8 in each group) was determined by measuring the relative density of each band on an immunoblot (4 different immunoblots with two samples from each group on each blot), normalized to the average control values on each blot. Each blot was first probed for pS1179eNOS, then stripped and re-probed for total eNOS. (B) Total eNOS normalized to the reference gene, ERK2. Relative eNOS values were normalized to relative ERK2. Denotes (*) significantly (P<0.05) greater than Control and Oxygen P15. Representative blots are shown above each graph with quantification (band density) shown below each band.*

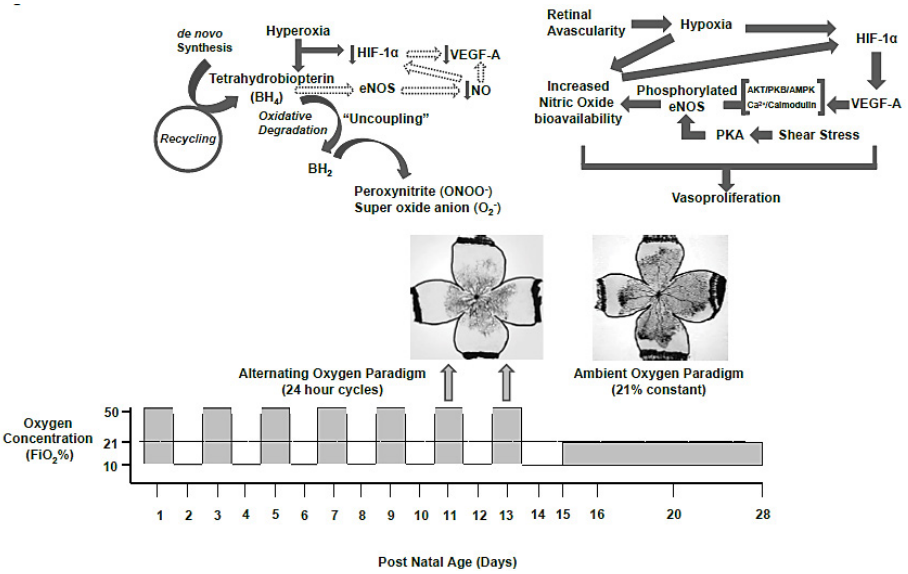

Figure 6. *speculative mechanism, that highlights the far-reaching implications for the role of NO in both the angio-inhibitory as well as the angio-proliferative phase of ROP.*

From our findings which demonstrate that both eNOS and VEGF164 overexpression correlate highly with the extent of neo-vasoproliferation during hypoxia, we postulate that NO bioavailability, more than the extent of avascularity is a key feature that governs the angioproliferative response to hypoxia (Figures 5 and 6).

Other studies have demonstrated the link between VEGF and NO, although there is lack of consensus as to whether the interplay promotes or antagonizes angiogenesis. We postulate that the link between VEGF and NO is such that there is feedback of regulation between the two and this hypothesis helps to explain the underlying biology of the complex angiogenic responses observed in the hyperoxic and hypoxic environments. In hyperoxia, we postulate "uncoupling" of NO which promotes peroxynitrite formation rather than NO and that the low bioavailability of NO fails to stimulate either HIF1-alpha expression or fails to stimulate VEGF expression indirectly or directly. In the hypoxic environment, high HIF1-alpha levels stimulate VEGF expression that stimulates phosphorylation of eNOS, thereby increasing NO bioavailability which can stimulate HIF1-alpha expression augmenting VEGF expression and providing a positive feedback mechanism that promotes dysregulated angiogenesis.

Although, our current study does not address vasoattenuation during hyperoxia, it is plausible that NO bioavailability could play a prominent role in that process as well. It is feasible that constant hyperoxic conditions or oscillations (50%/10% FiO_2) produce either a sustained or extensive suppression

of NO production, respectively, perhaps by depletion of the rate-limiting co-factor tetrahydrobiopterin (BH4) leading to eNOS uncoupling. This hypothesis is supported by Edgar et al. who used GTP cyclohydrolase (GTPCH)-depleted mice to demonstrate that hyperoxia diminished BH4 in the neonatal transgenic and wild-type retinas, resulting in reduced NOS function and increased reactive nitrogenous species leading to vessel closure [19]. Mechanistically, NOS uncoupling would result in production of super oxide anion (O_2^-) and peroxynitrite ($ONOO^-$) thereby promoting vessel constriction, closure and leading to regions of avascularity. The subsequent short period of room air hypoxia (4 days) might be insufficient to restore NO to levels that stimulate HIF-1 α and VEGF-A. Therefore, a response to a hypoxic stimulus stemming from avascularity would manifest as a blunted and delayed neovascular response, in agreement with the observations of Penn et al.

The observations by Penn et al. that the delta FiO_2 (difference between the two oxygen concentrations) is linearly and positively related to the extent of avascularity and that the higher the oxygen concentration level (relative to the hypoxia) the greater the area of avascularity are consistent with NOS suppression by hyperoxia. Additionally, the maintenance of a constant level of hyperoxia results in the greatest extent of avascularity [18]. These observations support the notion that the relationship between avascularity and oxygen could reside in depleted BH4 and a reduction in NO bioavailability as a consequence of hyperoxia.

Because our aim was to mechanistically investigate the vasoproliferative phase in this animal model, we did not delve into the molecular causes for the peripheral avascularity which remains an exciting area for future investigation. We propose a speculative mechanism (Figure 6) that highlights the far-reaching implications for the role of NO in both the angio-inhibitory as well as the angio-proliferative phase of ROP.

Although the interrelationship between eNOS and VEGF has been described in a variety of models and disease states, the relative contribution by each eNOS and VEGF to the angiogenic component in ROP has not been clearly elucidated. In this manuscript, we propose that NO biology is not only contributory, but central to the vascular anomalies that appear in the angio-inhibitory (speculative) as well as the angio-proliferative phase of ROP. This study provides temporal correlative data that demonstrate a progressive increase in phosphorylation of eNOS including mRNA and protein levels with elevations in VEGF mRNA and protein levels in the hypoxic phase of ROP that coincide with the extent of vasoproliferation. This relationship has not been previously elucidated in this ROP model and is of value in helping to discern the complex etiology of the angioproliferative mechanism operant in ROP.

Others have demonstrated that VEGF mRNA and protein levels in the rat OIR model are elevated during cycling oxygen levels and that specific isoforms are differentially affected, depending on the number of cyclic exposures [20]. Interestingly, VEGF levels are upregulated during the time course of retinal *avascularity,* suggesting the presence of an antagonistic regulatory molecule that might be pigment-epithelium derived factor (PEDF). However, the PEDF levels were not found to be significantly elevated [20].

Based on current understanding of NO biology and VEGF interaction, it is feasible that the vaso-arrest or vaso-attenuation could partially stem from a microenvironment that lacks vasoinduction signals for example suppression of NO bioavailability via uncoupling of eNOS during oxygen fluctuations leading to areas of avascularity. Therefore, a peripheral retina micro-environment exists that is slanted towards vaso-arrest irrespective of the elevated VEGF levels. This notion is supported by the finding that the eNOS overexpressing transgenic OIR mouse model exhibits an enhanced angioproliferative drive. During a five day hyperoxia exposure in the rat, the NOS inhibitor N-nitro-L-arginine "aggravated" the vasoobliteration and concomitantly decreased VEGFR2 expression [21], providing additional evidence for the role of NO in vasoobliteration during hyperoxia. However, direct extrapolation of those findings to the current animal model is hampered by the use of a different oxygen exposure regiment, 2 or 5 days at 80% oxygen, to induce the retinopathy in 7 day-old rats.

Our correlative data supports the mechanism that during the vasoproliferative phase of ROP we observe a concomitant increase in VEGF164 and a rise in the ratio of phosphorylated eNOS to total eNOS correlated with the extent of vasoproliferation. Although direct measurements of NO release were not conducted, we refer to the "bioactive eNOS" as the phosphorylated form of the synthase enzyme. The nomenclature of "bioactive eNOS" is synonymous with the phosphorylated form of the enzyme and this designation is widely accepted in the literature. It has been demonstrated that phosphorylation of the synthase at Serine1179 is a prerequisite for the activity of the enzyme and subsequent generation of NO.

Phosphorylated eNOS generates NO and the increased bioavailability of NO suggests that this apparent pro-angiogenic molecule contributes to the vaso-prolific hypoxic response of the retina. Hypoxia will also increase the half-life of NO and augment its bioavailability with the consequence that elevated NO could elevate VEGF expression. The combination of these two elements establishes a robust pro-angiogenic milieu that can promulgate the characteristic vasoproliferation, giving rise to vascular tufts and haemorrhaging at the interphase of the vascular and avascular regions of the retina. The relative contributions to the angioinductive signals stemming from the pro-angiogenic VEGF growth factor versus that from the bioactive phosphorylated eNOS during the vasoproliferative phase remains to be fully elucidated.

We utilized whole retinal homogenates to make determinations of pS1179eNOS/eNOS levels. This approach is warranted and appropriately represents vascular eNOS because eNOS protein expression by immunoreactivity has been demonstrated to be expressed *exclusively* in the endothelium of the developing rat retina [21,22]. However, retinal eNOS expression has been described to reside in non-vascular tissue and has been detected in retinal ganglion cell and inner nuclear layer neurons, but restricted to ischemia-reperfusion injury in a high intraocular pressure rat model [22]. The developing human retina also expresses non-vascular neuronal eNOS expression in amacrine and photoreceptor cells, but this appears to be minor when compared to blood vessel expression in these situations [22]. Although, our immunohistochemistry data exhibited localized

increases in eNOS immunoreactivity in agreement with increased eNOS mRNA determined by RT PCR, an overall increase in retinal eNOS protein was not obtained by Western Blot analysis when normalized to the *ERK2* gene. However, the bioactive eNOS as determined by phosphorylation at Ser1179 was significantly increased during the vasoproliferative phase of ROP. We interpret our data to suggest that a concomitant elevation of VEGF and phosphorylated NOS facilitate the emergence of a vasoproliferative environment in the retina. These findings are in agreement with the findings that NO is pro-angiogenic in the retina, as described in Ando et al. and Edgar et al. [23].

For future studies, it would be intriguing to explore whether the phosphorylation of eNOS, in the vasoproliferative phase of ROP, is mediated by VEGF. Others have demonstrated that VEGF stimulated phosphorylation of eNOS via an Akt dependent mechanism [24]. VEGF increases Akt phosphorylation, thereby providing a functional link to evoke downstream mitogenic signaling relevant to the angiogenic process. Phosphorylation of AktT308 and AktS474 has been shown to activate the kinase under the influence of VEGF growth factor signaling. This appears to be mediated by cyclin A or mTORC2 [25,26] and a dual mTOR kinase inhibitor demonstrates inhibition of Glomeruloid formation in an IOR mouse model [27]. Other protein kinases besides Akt have been implicated in phosphorylation of eNOS serine1179 and these include PKA, PKC, PKG and AMP kinase [28].

Many of the salient features of the microangiopathy observed in the vasoproliferative phase of ROP might be linked to dysregulation or alterations in NO biology. Local vascular tone and regulation of blood flow in the neonatal retina could be partially mediated by the contractility of pericytes, which have been shown to change their contractile tone in response to NO. Hypoxia augments the extent of pericyte relaxation in the presence of a nitric oxide donor [29] and hypoxia increases pericyte relaxation via guanylate cyclase NO-mediated pathway [30]. Haemorrhaging of the retina upon neovascularization could stem not only from NO and prostacyclin mediated VEGF-induced vascular leakage [28], but from impaired autoregulatory capacity. Previous studies in other species have demonstrated that NO partially influences the autoregulatory ability of the neonatal retinal vasculature [31-33]. Additionally, feed-forward neurovascular coupling, in which active neurons release signaling molecules, leads to vasodilation involving NO modulatory mechanisms that influence blood flow regulation in the retina [34]. It is noteworthy to mention the evolution of understanding of operant mechanisms in the field of ROP in the context of the Third International Symposium on Retinopathy of Prematurity held November 2003 in Anaheim, California. In that meeting, there was no mention of, suggested role for, or speculation of the possibility of NO physiology involved in the pathogenesis of retinopathy of prematurity [35,36]. The potential involvement of NO as a significant factor in the etiology of retinopathy of prematurity has only come to be recognized within the last 13 years. The insights gained from this and prior studies contribute to the understanding of key elements that regulate the dynamics of the vascular changes observed in ROP and may aid in the elucidation of novel, relevant metabolic pathways that suggest therapeutic targets for the future management of ROP.

Acknowledgements

The authors express their gratitude to Dr. John Penn for his valuable guidance in the implementation of the animal model, serving as a consultant on the grant that partially funded this study and for insightful review of this manuscript. This study was partially supported by the Commonwealth Health Research Board (CHRB), Richmond, Virginia awarded to AH (PI), JLJ, FAL and R.L.W. (co-investigators). R.L.W. supported by NIH-R15HL102742-01 and Women in Scientific Education (WISE) grant from the National Science Foundation awarded to the College of William & Mary.

Disclosures

The authors declare that there is no conflict of interest regarding the publication of this paper, no secondary interest nor financial gain.

References

1. Pierce EA, Foley ED. Smith LEH. Regulation of vascular endothelial growth factor by oxygen in a model of retinopathy of prematurity. Arch Ophthalmol. 1996;114(10):1219-28.
2. Forsythe JA, Jiang B-H, Iyer NV, et al. Activation of vascular endothelial growth factor gene transcription by hypoxia-inducible factor. Mol and Cell Biol. 1996;4604-13.
3. Fischer S, Clauss M, Wiesnet M, et al. Hypoxia induces permeability in brain microvessels endothelial cells via VEGF and NO. Am J Physiology. 1999;276:C812-20.
4. Kimura H, Esumi H. Reciprocal regulation between nitric oxide and vascular endothelial growth factor in angiogenesis. Acta Biochim Pol. 2003;50(1):49-59.
5. Ando A, Yang A, Mori K, et al. Nitric oxide is proangiogenic in the retina and choroid. J Cell Physiol. 2002;191(1):116-24.
6. Li W, Du D, Wang H, et al. Silent information regulator 1 (SIRT1) promotes the migration and proliferation of endothelial progenitor cells through the PI3K/Akt/eNOS signaling pathway. Int J Clin Exp Pathol. 2015;8(3):2274-87.
7. Michell BJ, Chen Zhi-ping, Tiganis T, et al. Coordinated control of endothelial nitric-oxide synthase phosphorylation by protein kinase C and the cAMP-dependent protein kinase. J Bio Chemistry 2001;276(21):17625-628.
8. Ma J, Mehta M, Lam G, et al. Influence of sub-retinal fluid in advanced stage retinopathy of prematurity on proangiogenic response and cell proliferation. Molecular Vision. 2014;20:881-93.
9. Barnett JM, Yanni SE, Penn JS. The development of the rat model of retinopathy of prematurity. Doc Ophthalmol 2010;120(1):3-12.
10. Roberto KA, Tolman BL, Penn JS. Long-term retinal vascular abnormalities in an animal model of retinopathy of prematurity. Curr Eye Res. 1996;(9):932-37.
11. Lutty GA, McLeod DS. A new technique for visualization of the human retinal vasculature. Arch Ophthalmol. 1992;110(2):267-76.
12. Lutty GA, McLeod DS. Phosphatase enzyme histochemistry

for studying vascular hierarchy, pathology, and endothelial cell dysfunction in retinal and choroid. Vision Res. 2005;45:3504-11.

13. Fang J, Yan L, Shing Y, Moses MA. HIF-1α-mediated up-regulation of vascular endothelial growth factor, independent of basic fibroblast growth factor, is important in the switch to the angiogenic phenotype during early tumorigenesis. Cancer res. 2001;61:5731-5.
14. Looft-Wilson RC, Ashley BS, Billig JE, et al. Chronic diet-induced hyper homocysteinemia impairs eNOS regulation in mouse mesenteric arteries. Am J Physiol Regul Integr Comp Physiol. 2008;295(1):R59-66.
15. Rocha-Martins MB, Njaine B, Silveira MS. Avoiding pitfalls of internal controls: Validation of reference genes for analysis of qRT-PCR and western blot throughout rat retinal development. PLoS One. 2012;7:e43028.
16. Semenza GL. Physiology regulation of oxygen homeostasis by hypoxia-inducible factor 1. 2008;24:97-106.
17. Mowat FM, Luhmann UFO, Smith AJ, et al. PLosOne. HiF-1alpha and HIF-2alpha are differentially activated in distinct cell populations in retinal ischaemia. 2010;5(6):e11103.
18. Penn JS, Tolman BL, Henry MM. Oxygen-induced retinopathy in the rat: Relationship of retinal nonperfusion to subsequent neovascularization. Investigative Ophthalmol Vis Sci. 1994;35(9):3429-35.
19. Edgar KS, Matesanz N, Gardiner TA, et al. Tetrahydrobiopterin levels in the neonatal retina implications for nitric oxide synthase function in retinopathy. The Am J Path. 2015;185:6.
20. Beauchamp MH, Sennlaub F, Speranza G, et al. Redox-dependent effects of nitric oxide on microvascular integrity in oxygen-induced retinopathy. Free Radic Biol Med. 2004;37(11):1885-94.
21. Cheon EW, Park CH, Kang SS, et al. Change in endothelial nitric oxide synthase in the rat retina following transient ischemia. Neuroreport. 2003;14(3):329-33.
22. Edgar K, Gardiner TA, van Haperen R, et al. eNOS overexpression exacerbates vascular closure in the obliterative phase of OIR and increases angiogenic drive in the subsequent proliferative stage. Invest Ophthalmol Vis Sci. 2012;53(11):6833-50.
23. McColm JR, Geisen P, Hartnett ME. VEGF isoforms and their expression after a single episode of hypoxia or repeated fluctuations between hyperoxia and hypoxia: Relevance to clinical ROP. Molecular Vision. 2007;10:512-20.
24. Fulton D, Gratton JP, McCabe TJ, et al. Regulation of endothelium-derived nitric oxide production by the protein kinase Akt. Nature. 1999;399(6736):597-01.
25. Liu P, Begley M, Michowski W, et al. Cell-cycle-regulated activation of Akt kinase by phosphorylation at its carboxyl terminus. Nature. 2014;508:541-45.
26. Sarbassov DD, Guertin DA, Ali SM, et al. Phosphorylation and regulation of Akt/PKB by the rictor-mTOR complex. Science. 2005;307(5712):1098-101.
27. Jacot JL, Sherris D. Potential therapeutic roles for inhibition of the PI3K/Akt/mTOR Pathway in the Pathophysiology of Diabetic Retinopathy. J Ophthalmol. 2011, Article ID 589813.
28. BooYC, Sorescu G, Boyd N, et al. Shear stress stimulates phosphorylation of endothelial nitric-oxide synthase at Ser1179 by Akt-independent mechanisms: Role of protein kinase A. J Bio Chem. 2002;277(5):3388-96.
29. Haefliger IO, Anderson DR. Oxygen modulation of guanylate cyclase-mediated retinal pericyte relaxations with 3-morpholino-sydnonimine and atrial natriuretic peptide. Investigative Ophthalmology Vis Sci. 1997;38(8):1563-68.
30. Haefliger IO, Chen Q, Anderson DR. Effect of oxygen on relaxation of retinal pericytes by sodium nitroprusside. Graefes Arch Clin Exp Ophthalmol. 1997;235(6):388-92.
31. Murohara T, Horowitz JR, Silver M, et al. Vascular endothelial growth factor/vascular permeability factor enhances vascular permeability via nitric oxide and prostacyclin. Circulation.1998;97(1):99-107.
32. Jacot JL, O'Neill JT, Scandling DM, et al. Nitric oxide modulation of retinal, choroidal, and anterior uveal blood flow in newborn piglets. J Ocul Pharmacol Ther. 1998;5:473-89.
33. Newman EA. Functional hyperemia and mechanisms of neurovascular coupling in the retinal vasculature. J cerb blood flow meta. 2013;33:685-95.
34. Lutty GA, Chan-Ling T, Phelps DL, et al. Mol Vis. Proceedings of the third international symposium on retinopathy of prematurity: An update on ROP from the lab to the nursery (November 2003, Anaheim, California). 2006;12:532-80.
35. Li S, Tay D, Shu S, et al. Endothelial nitric oxide synthase is expressed in amacrine cells of developing human retinas. Invest Ophthalmol Vis Sci. 2006;47(5):2141-9.
36. Penn JS, Henry MM, Wall PT, et al. The range of PaO_2 variation determines the severity of oxygen-induced retinopathy in newborn rats. Invest Ophthalmol Vis Sci. 1995;36(10):2063-70.

***Correspondence to:**

Jorge L Jacot
Department of Pathology and Anatomy
Eastern Virginia Medical School
USA
Tel: +17574465600
E-mail: JacotJL@EVMS.edu